Computation of Radiation from Wire Antennas on, or near, Conducting Bodies of Translation

Nabeel Abbas Areebi

Dept. of Physics, College of Education, Univ. of Qadisiya, Iraq.
nabeelabbasph@yahoo.com

Abstract:

A method of moments (MM) formulation is presented for active and passive wire radiators attached to, or near, bodies of translation(BOT), including open or closed cylinders of arbitrary cross section as well as curved panels. This formulation builds on previous MM analysis for BOT's and wires. The analysis incorporates a special junctions basis set for the antenna attachment points. Total domain and piecewise continuous expansion functions are used on the surfaces. The formulation is primarily intended for prediction of radiation patterns of wire antenna (such as monopoles and loops) on asymmetric bodies of translation, open or closed(capped). Fortran Power Station 90 was used to programming. Radiation patterns are plotted by origin program.

Keywords: method of moments, body of translation, radiation patterns, the junction problem.

حساب هيكل الإشعاع لسلك على سطوح الأجسام الموصلة والمتولدة انتقاليا او بالقرب منها

نبيل عباس عريبي

قسم الفيزياء – كلية التربية – جامعة القادسية

الخلاصة:

اعتمدنا الصيغة الرياضية لطريقة العزوم لحساب الاشعاعات الناتجة عن سلك مثبت بالقرب من سطح موصل متولد انتقاليا كأسطوانات مفتوحة او مغلقة محكمة المقطع العرضي او صفائح منحنية . تعتمد صيغة المعادلات في هذا البحث على التحليل الرياضي الخاص بحالات ارتباط سلك بالأجسام الموصلة والمتولدة انتقاليا بما في ذلك المعادلات التي تصف نقاط ارتباط الهوائي بالسطح والدوال الرياضية التي تصف المجال الكلي على سطوح تلك الاجسام . من خلال تلك المعادلات وجدت الهياكل الاشعاعية للهوائي السلكي سواء كان سلك واحد او مجموعة اسلاك موجودة على سطوح الاجسام المتولدة انتقاليا المفتوحة او الصلدة . استخدمنا لغة الفورتران ٩٠ لبرمجة تلك المعادلات ، في حين استخدم برنامج origin لرسم المخططات او الهياكل الاشعاعية.

الكلمات المفتاحية: طريقة العزوم ، الجسم المتولد انتقاليا، هياكل اشعاعية، مسائل الارتباط.

1. Introduction

The analysis methods for antennas are based on equivalent magnetic current distribution around the patch edges (similar to slot antennas). The popular analytical techniques such as transmission-line model, which described the microstrip radiator element as a transmission line resonator with no transverse field variations[1].

The moment method, which depend on the surface currents are used to model the microstrip patch, and volume polarization currents in the dielectric slab are used to model the fields in the dielectric slab. An integral equation is formulated for the unknown currents on the microstrip patches and the feed lines and their images in the ground plane[2].

The earliest application of the method of moments (MM) was used for the analysis of thin wire radiators and scatters .Recent investigators [3]-[4] have used the MM technique to examine such radiators on or near bodies of revolution (BOR).In many real-world situations involving aircraft and spacecraft ,the principle physical features of the antenna platform adjacent to the antenna feed point often can be modeled as a BOR. Often the electrical size of the body to which the antenna is attached is comparable to a few wavelengths (λ). In these cases , the entire structure is coupled closely to the antenna elements, so the whole configuration becomes a radiator . To analyze such configurations requires incorporation of complex boundary conditions in the electromagnetic formulation used. The MM technique is the most appropriate analytical tool for such problems.

To extend the usefulness of the MM analysis for a significantly broader class of radiating platforms, I developed a MM formulation for wire antennas attached to, or near , finite asymmetric surfaces formed by a generating curve translated along an axis. For brevity , such surfaces are denoted as bodies of translation(BOT) in analogy to the earlier work for bodies of revolution [3]-[4]. Subclasses of BOT include finite cylindrical bodies of arbitrary cross section either open or capped. In practice, aircraft wings and fuselages can often be approximated as BOT's. An interesting limiting case of BOT's are flat or curved plates. An earlier BOT formulation treated the scattering from such surfaces [5].

Previously , a MM formulation using a wire was used to treat asymmetric bodies. However, the computer resources necessary to carry out such an analysis are often prohibitive and limit its general use. A simple analytical treatment is proposed here allowing substantial configuration flexibility for both the antennas and the surfaces on which they are located. The theoretical development parallels in part the MM/BOR-wire [4] and MM/BOR [6] formulations. While the primary motivation for our investigations is the efficient analytical treatment of antennas on or near BOT's, the results are extended easily to the scattering from such configurations. For examples of the MM/BOR – wire formulation applied to scattering[7].

2. Theory background

The electromagnetic radiated or scattered fields are expressed in terms of potentials from which a general integral equation for the surface currents on the radiating or scattering body can be obtained. For maximum generality and unity of treatment , the electric field integral equation (EFIE) formulation is chosen over the magnetic field formulation

(MFIE) for the currents on both the off-surface wire radiators and the BOT surface. For this discussion , the generic configuration shown in Fig.(1)a is used . The overall (closed) body is composed of a surface formed by an arbitrary generating curve translated along the z-axis, denoted as the BOT. The BOT can be terminated by planar end caps with tangents normal to the z-axis. The requirement of planar caps is introduced to simplify the subsequent discussion and can be removed if desired. The vicinity of the antenna attachment point is designated as the junction region, consisting of a small annular disk on the BOT and wire attachment segment on the antenna nearest the BOT surface. Imposing the usual boundary conditions on the perfectly conducting surfaces in Fig. 1(a), the generalized EFIE expressed in terms of integro-differential operators $L(\cdot)$ on the BOT, caps, wire, junction, and edge region is given by:

$$\vec{E}_{\tan}^{inc} = L_s(\vec{J}) + L_c(\vec{J}) + L_w(\vec{J}) + L_j(\vec{J}) + L_e(\vec{J}) \quad .....(1)$$

where $(\vec{E}_{\tan}^{inc})$ denotes the tangential component of the impressed fields on each of the various surfaces (or regions) in Fig. 1(a), due to the antenna feed voltage . The operator L_s refers to the BOT surface S_s and is given by[8]

$$L_s = \left[j\omega\mu \iint_{S_s} \vec{J}\phi ds' - \frac{1}{j\omega\varepsilon} \nabla_s \iint_{S_s} (\nabla_s' \cdot \vec{J})\phi ds' \right]_{\tan} \quad .....(1a)$$

where the free-space Green's function is $\phi = \dfrac{e^{-jkR}}{4\pi R}$, $\vec{J}$ denotes the surface current density on S_s, R is the distance from a source to a field point , ∇_s' is the surface gradient on the BOT defined subsequently, ω is the radian frequency. and μ and ε are the permeability and permittivity of the medium, respectively. For the caps, the operator $L_c(*)$ is identical to $L_s(*)$, except the domain of integration spans the caps. Similarly, the operator $L_e(*)$ is identical to $L_s(*)$, except the domain of integration spans the edge region on either the BOT or the caps. Analogously for the wire part,

$$L_w(J) = j\omega\mu \int_{wire} \vec{J}\phi dh' - \frac{1}{j\omega\varepsilon} \vec{u}_w \frac{d}{dh} \int_{wire} \frac{d\vec{J}}{dh'} \phi dh' \quad .....(1b)$$

Where $L_w(*)$ is the one –dimensional operator on the total wire current in the thin wire approximation and u_w is a unit

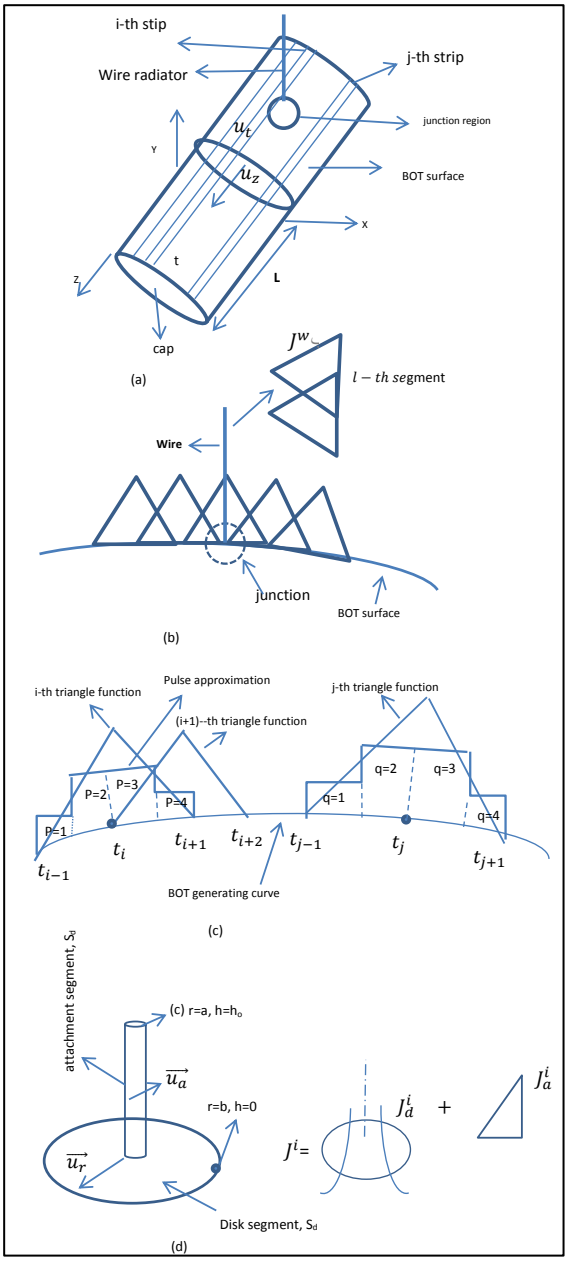

Fig. 1 (a) Generic BOT-wire geometry . (b) Enlargement of BOT- wire attachment region. (c) Pulse approximation for triangle functions on BOT surface. (d) Junction region representation.[8]

vector along the wire. The operator in the junction region $L_j(*)$ is $L_w(*)$, when the domain of integration is restricted to the attachment segment S_a, $L_j(*)$ is $L_s(*)$ when the surface integration is confined to the disk part of the junction region S_d (Figs. 1(b) and 1(d)).

To solve (1) for the unknown $\vec{J}$ on the entire surface, explicit expressions must be obtained for all operators . I used the Galerkin (MM) technique to expand the currents specific to each region, subdividing the curved BOT surface into axial strips, the caps into trapezoidal patches, the wire radiators into connected straight-wire segments, the junction region into an attachment and a disk part, and the edge region into patches on the BOT and the caps. A set of basis and testing functions for the unknown currents in each of these regions is introduced. The basis sets for the wires and the junctions are identical to those in [4]

3. Calculating Basic Functions for the Currents

First, the expansion of the currents on the BOT surface is considered. The two orthogonal components of the surface currents on the BOT. i.e., $\vec{J}^{st}$ and $\vec{J}^{sz}$, are expanded in terms of a total domain expansion along Z and in overlapping triangle functions along the t-direction (Fig. 1(c)). Specifically, the currents on the i-th axial segment of the BOT in terms of the unknown coefficients I_{ni}^{st} and I_{ni}^{sz} are:

$$\vec{J}_i^s = \sum_{n=0}^{\pm N} (I_{ni}^{st}\vec{J}_{ni}^{st} + I_{ni}^{sz}\vec{J}_{ni}^{sz}) \quad (A/m) \ldots . (2)$$

Where

$$\vec{J}_{ni}^{s\alpha} = \vec{u}_\alpha f_l^\alpha(t) v_n^\alpha(z), \quad \alpha = t \; or \; z \quad \ldots (2a)$$

And

$$v_n^\alpha(z) = \begin{cases} \exp\left(\frac{jn\pi z}{L}\right) & \alpha = t \\ \exp\left(\frac{jn\pi z}{L}\right) - (-1)^n & \alpha = z \end{cases} \quad \ldots (2b)$$

Where N is the largest mode considered, L is the half-length of the BOT, $\vec{u}_\alpha$ is a unit vector along the BOT, and the i-th surface triangle function $f_l^\alpha(t)$ is defined as :

$$f_l^\alpha(t) = \begin{cases} 1 - |\acute{t}|, & |\acute{t}| \le 1 \\ 0, & |\acute{t}| > 1 \end{cases}, \; \acute{t} = t - t_i \quad \ldots 2c$$

Generally, ten triangle functions per λ yield accurate results. (The axial component of current $\vec{J}_{ni}^{sz}$ is chosen to vanish at the ends of the BOT.).

The cap surface is parameterized by $\rho = r/\acute{r}\,(\emptyset)$ and t , where r is the distance from the cap origin to any point on the cap; $\acute{r}(\emptyset)$ is the radial distance from the cap origin to the cap rim; t is the distance along the rim (see Fig. 2). Note the cap surface is mapped onto the rectangle $\{0 \le \rho \le 1, 0 \le t \le t_{max}\}$ by this parameterization. The currents are expanded in terms of the two components along $\vec{u}_t$ and $\vec{u}_\rho$, yielding for the l-th trapezoidal patch

$$\vec{J}_l^c = \vec{u}_t I_l^{ct} J_l^{ct} + \vec{u}_\rho I_l^{c\rho} J_l^{c\rho} \quad (A/m) \quad \ldots . (3)$$

Where

$$\vec{J}_l^{c\alpha} = f_l^\alpha(t) g_l^\alpha(\rho), \quad \alpha = t \; or \; \rho \quad \ldots (3a)$$

and $f_l^\alpha(t)$ and $g_l^\alpha(\rho)$ are overlapping triangle functions spanning the cap surface in the t and ρ directions, respectively. (In general, $\vec{u}_t \cdot \vec{u}_\rho \neq 0$).For maximum flexibility in surface representation, the patches are allowed to be nonuniform so that the triangle functions can vary from patch to patch. (For alternate patch representations,[9] and [10]).

junction currents are the same as in [4], and for completeness, they are repeated here. On the l-th wire segment,

the filamentary wire current can be expressed as

$$\vec{J}_l^{\,w} = \vec{u}_l^{\,w} I_l^w T_l(h) \quad (A), \qquad \ldots.(4)$$

where $\vec{u}_l^{\,w}$ is a unit vector along the l-th segment, $T_l(h)$ denoted a triangle function (Fig. 1(b)), and I_l^w is the unknown wire-current coefficient associated with the l-th segment. For a wire segment nearest the attachment point, one-half of a wire triangle function overlaps the half-triangle basis term on the attachment segment. This representation yields a piecewise continuous (pc) current from the junction to the wire.

The junction current $\vec{J}^j$, in terms of basis functions associated with the wire attachment segment S_a and the disk region S_d, is given as

$$\vec{J}^j(\rho) = \vec{I}^j \begin{cases} \vec{J}_a^j, & \rho \in S_a \\ \vec{J}_d^j, & \rho \in S_d \end{cases} \quad (A/m) \quad \ldots(5)$$

where

$$\vec{J}_a^j = \vec{u}_a \frac{T_a(h)}{2\pi a}, \qquad \ldots.(5a)$$

$$\vec{J}_d^j = -\vec{u}_r \frac{1}{2\pi r}\left(\frac{b-r}{b-a}\right), \qquad \ldots.(5b)$$

and $\vec{u}_a$ and $T_a(h)$ are an outward-directed unit vector and a half-triangle function on the attachment segment, retrospectively; $\vec{u}_r$ is an unit vector on the (annular) disk surface away from the wire, r is the radial distance on the disk, b is the outer disk radius, a is the wire radius, and $\vec{I}^j$ is the unknown junction current coefficient. A similar formulation for the junction currents is given in [11] and [12].

The edge region spans the rims of the caps (S_c) and the ends of the BOT surface (S_s) (Fig. 2(b)). The edge currents are defined as

$$\vec{J}_l^e(\rho) = I^e \begin{cases} \vec{J}_l^{ce}, & \rho \in cap\ edge\ patch \\ \vec{J}_l^{se}, & \rho \in BOT\ edge\ patch \end{cases} \quad (A/m) \quad \ldots(6)$$

where

$$\vec{J}_l^{ce} = \vec{u}_\rho f_l^\rho(t) h_l^\rho(\rho) \qquad \ldots\ldots(6a)$$

and in the neighborhood of the edge at $z = \pm L$,

$$\vec{J}_l^{se} = \pm\vec{u}_z f_l^z(t) h_l^z(z) \qquad \ldots\ldots(6b)$$

and $h_l^\rho(\rho)$ and $h_l^z(z)$ denote half-triangle functions on the cap and BOT edge regions, respectively. (The t-components of the currents in the edge region are contained in the expansion set for $\vec{J}^{ct}$ and $\vec{J}^{st}$).

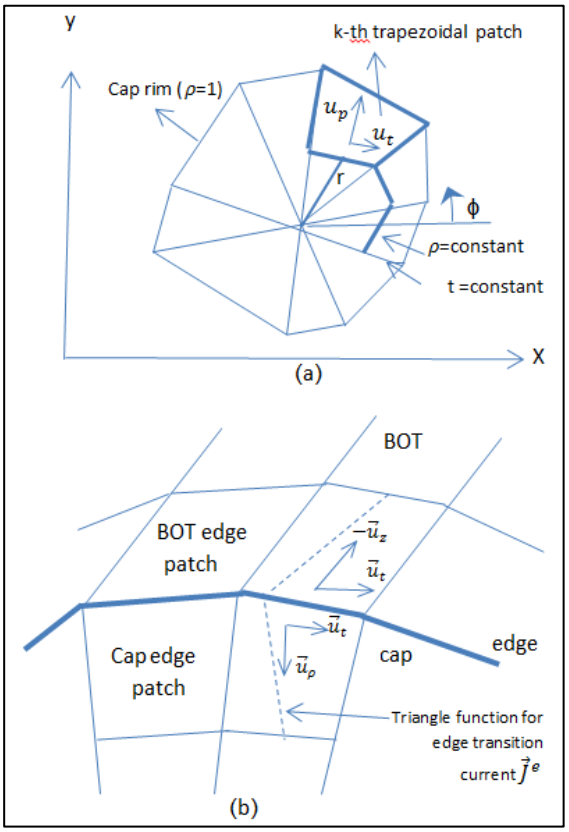

Fig. 2. Cap and edge geometry. (a) Cap coordinates . (b) Detail of edge region

4. Impedance Expressions

The expansions for the current on the BOT surface, the caps, the wire segments, the junction, and the edge regions, given in [2]-[6] are substituted into (1). The inner products of the integral operators L(*) in (1) are formed with the testing functions ($\vec{w} = \vec{J}^*$) via the Galerkin method, where the asterisk denoted the conjugate operator. A system of linear equations for the unknown current coefficients, $I_{ni}^{st}, I_{ni}^{sz}, I_l^{ct}, I_l^{c\rho}, I_l^w, I^j \; and \; I^e$, written in matrix form is

$$\begin{bmatrix} Z_{-N,-N}^{ss} & \cdots & \cdots & \cdots & Z_{-N,-N}^{ss} & \vdots & Z_{-N}^{sw} & Z_{-N}^{sj} & Z_{-N}^{sc} & Z_{-N}^{se} \\ \vdots & \cdots & Z_{-N,-N}^{ss} & \cdots & \cdots & \vdots & Z_0^{sw} & Z_0^{sj} & Z_0^{sc} & Z_0^{se} \\ Z_{-N,-N}^{ss} & \cdots & \cdots & \cdots & Z_{-N,-N}^{ss} & \vdots & Z_N^{sw} & Z_N^{sj} & Z_N^{sc} & Z_N^{se} \\ \cdots & \cdots & \cdots & \cdots & \cdots & \vdots & \cdots & \cdots & \cdots & \cdots \\ Z_{-N}^{ws} & \cdots & Z_0^{ws} & \cdots & Z_N^{ws} & \vdots & Z^{ww} & Z^{wj} & Z^{wc} & Z^{we} \\ Z_{-N}^{js} & \cdots & Z_0^{js} & \cdots & Z_N^{js} & & Z^{jw} & Z^{jj} & Z^{jc} & Z^{je} \\ Z_{-N}^{cs} & \cdots & Z_0^{cs} & \cdots & Z_N^{cs} & \vdots & Z^{cw} & Z^{cj} & Z^{cc} & Z^{ce} \\ Z_{-N}^{es} & & Z_0^{es} & \cdots & Z_N^{es} & & Z^{ew} & Z^{ej} & Z^{ec} & Z^{ee} \end{bmatrix}$$

$$\begin{bmatrix} I^s \\ \cdots \\ I^w \\ I^j \\ I^c \\ I^e \end{bmatrix} = \begin{bmatrix} V^s \\ \cdots \\ V^w \\ V^j \\ V^c \\ V^e \end{bmatrix} \qquad \text{.....(7)}$$

The right column vector above represents a generalized voltage vector, and the Z elements are the familiar impedances defining the EM interactions between various parts of the body in Fig. 1(a). For example, the BOT-surface interactions are given by Z_{mn}^{ss} . Similarly, the cap-cap, BOT-cap, wire-wire, BOT-wire, BOT-junction, wire-junction and the junction-junction interactions are defined by $Z^{cc}, \; Z_m^{sc}, \; Z^{ww}, \; Z_m^{sw}, Z_m^{sj}, \; Z^{wj} \; and \; Z^{jj}$, respectively.

The elements in (7) with e superscripts refer to the edge interactions. The composition of the system matrix in (7) is determined by the particular configuration under analysis. For example, if the radiating (or parasitic) wire element in Fig. 1(a) is not attached to the BOT surface (i.e., as in the case of radiative coupling), the junction-related elements can be deleted from the system matrix (7).Similarly, if there are no wire antenna on the BOT, the system matrix contains only elements of $Z_{mn}^{ss}, \; Z^{cc}, \; Z_m^{sc}$, and the edge related elements.

Specific analytical expressions for the various matrices in (7) can be obtained by evaluating the inner products having the form

$$Z = \langle \vec{w}, L(\vec{J}) \rangle =$$

$$\iint_s ds \iint_{\acute{s}} d\acute{s} \cdot j\square k \left[\vec{w} \cdot \vec{J} - \frac{1}{k^2} (\nabla \cdot \vec{w})(\acute{\nabla} \cdot \vec{J}) \right] \emptyset \quad \ldots (8)$$

where all superscripts and subscripts on $\vec{w}$ and $\vec{J}$ are omitted for simplicity and S and $\acute{S}$ refer to surface containing that field and source points, respectively; $\square = \sqrt{\mu/\epsilon}$ and $k = 2\pi/\lambda$. To evaluate (8), explicit forms for the divergence must be obtained. For any vector $\vec{A}$ on the BOT surface it can be shown that $\nabla \cdot \vec{A} = (\frac{\partial A_t}{\partial t} + \frac{\partial A_z}{\partial z},$ and similarly on the caps,

$$\nabla \cdot \vec{A} = (1/\rho)(\frac{\partial A_t}{\partial t}) + \frac{\partial A_\rho}{\partial r} + \frac{A_\rho}{r} .$$

The divergence terms for the junction current are given in [4]. Using the foregoing divergence expressions and the various expansion functions in (2)-(6), (9) can be evaluated for each of the regions of the generic BOT-wire configuration in Fig. 1(a). The detailed derivation is given in [13]. Only the formal definitions and summary of results are presented here.

5. Junction- Independent Impedance Elements

The BOT interaction matrix Z_{mn}^{ss} can be partitioned into submatrices

corresponding to the t and z ditected current components, i.e..

$$Z_{mn}^{ss} = \begin{bmatrix} Z_{mn}^{ss,tt} & \vdots & Z_{mn}^{ss,tz} \\ \dots & \dots & \dots \\ Z_{mn}^{ss,zt} & \vdots & Z_{mn}^{ss,zz} \end{bmatrix} \quad \text{.....(9)}$$

The (i,j)th element of these submatrices is obtained from

$$Z_{mn,ij}^{ss\alpha\beta} = \langle \vec{w}_{mi}^{s\alpha} \; L_s\left(\vec{J}_{nj}^{s\beta}\right)\rangle, \quad \text{....(10)}$$

where α, β are combinations of t and z, and m and n are the mode numbers of the axial expansion (2b); $\vec{w}_{mi}^{s\alpha}$ and $\vec{J}_{nj}^{s\beta}$ are the i-th testing and the j-th current basis functions, respectively, on the BOT surface. Z_{mn}^{ss} , summarized in Table 1, [8], is canonically similar to the system matrix arising from the MM analysis for BOR's [6]. However, the set of expansion functions used here is not orthonormal with respect to $L_s(*)$ as in the BOR case, and thus there is no modal decoupling. Hence all Z_{mn}^{ss} matrices are present, not just the diagonal ones. However, certain symmetries exist for G_{mn} and Z_{mn}^{ss} that reduce the full-time of the matrix. Specifically, $G_{mn} = (G_{mn})_t$, $Z_{mn}^{ss,tt}$ $=\left(Z_{mn}^{ss,tt}\right)_t, m_t(Z_{mn}^{ss,tz})=-n\left(Z_{mn}^{ss,zt}\right)$, and $Z_{mn}^{ss,zz} = (Z_{mn}^{ss,zz})_t$, where $(A)_t$ denotes the transpose of A. In the implementation of the analysis, only the lower triangular quadrant of Z^{ss} is computed, i.e., the partitioned submatrices are field for $0 \le m \le N$, and $-m \le n \le m$. The entire Z^{ss} matrix can be filled using the following modal symmetries:

$$Z_{mn}^{ss,tt} = \left(Z_{nm}^{ss,tt}\right)_t = Z_{-m,-n}^{ss,tt} = \left(Z_{-n,-m}^{ss,tt}\right)_t$$

$$Z_{mn}^{ss,zt} = -\left(Z_{nm}^{ss,tz}\right)_t = -Z_{-m,-n}^{ss,zt} = \left(Z_{-n,-m}^{ss,tz}\right)_t$$

$$Z_{mn}^{ss,tz} = -\left(Z_{nm}^{ss,zt}\right)_t = -Z_{-m,-n}^{ss,tz} = \left(Z_{-n,-m}^{ss,zt}\right)_t$$

$$Z_{mn}^{ss,zz} = (Z_{mn}^{ss,zz})_t = Z_{-m,-n}^{ss,zz} = \left(Z_{-n,-m}^{ss,zz}\right)_t$$

The matrix fill times for each impedance element in the MM/BOR and MM/BOT formulations are comparable. Detailed examination of the $G_{mn}(i,j)$ function shows that it is maximum when m=n and i=j, i.e., the largest values occur on the main diagonal of the Z^{ss} matrix, and the self-terms contribute the most. These properties lead to a diagonally strong overall matrix.

The (i,j)th element of the BOT-wire interaction matrix Z_m^{sw}, partitioned in to t and z components and defined as

$$Z_{m,il}^{sw,\alpha} = \langle \vec{w}_{mi}^{s\alpha} \; L_w\left(\vec{J}_l^{w}\right)\rangle, \; \alpha = t \; or \; z \quad \text{.(11)}$$

are given in Table 1.

The wire-wire interaction matrix elements Z_{kl}^{ww}, are listed in Table 2,[7]. Similar expressions can be derived for the cap interaction matrix Z^{cc}, partitioned into t and ρ (=polar coordinate) components depicted in Fig. 2(a). These as well as the remaining junction –independent matrix elements are derived in [10]. Brevity products their reproduction here.

6. Junction- Dependent Impedance Elements

The derivation of the junction-dependent impedance elements parallels the development in [4] for junction effects on BOR surface. This discussion is limited to a synopsis of its extension to BOT geometries. The junction element Z^{ij} is considered first. Referring to (5), the junction basis function consists of a disk term and a wire attachment term. The planar annular disk patch S_d is assumed to approximate the BOT surface at the junction point (Fig. 1(d)). This assumption is satisfactory when the disk radius b is much less than the BOT radius of curvature R at the attachment point (i.e., $b \ll R$) and the disk diameter is small compared to a wavelength. In practice, the latter condition is always met since the

disk diameter is taken to be the width of a BOT surface triangle function (i.e., usually $< 0.1\lambda$ in width). Analytical predictions using this approach correlate satisfactory with measured data even for input impedances, confirming the efficacy of the approximation. The expressions for $Z^{ij} and\ Z_l^{wj}$ are given in Table 1, [4].

The BOT-junction impedance elements are given by

$$Z_{mi}^{sj,\alpha} = \langle \vec{w}_{mi}^{s\alpha}, L_j(\vec{J}_a^j)\rangle + \langle \vec{w}_{mi}^{s\alpha}, L_j(\vec{J}_d^j)\rangle \quad \ldots.(12)$$

where $\alpha = t\ or\ z$, m is the mode number, and $\vec{w}_{mi}^{s\alpha}$ is the testing function associated with the i-th BOT axial strip. The first term in (12) is obtained from $Z_m^{sw\alpha}$ (see Table 1[12]) by replacing T_r by a half-triangle on the wire segment nearest the BOT. Explicit forms for the second term (disk part) of (12) are listed in Table 2[13]. The junction-BOT matrix elements are obtained from $Z_{n,i}^{js,\alpha} = Z_{-n,i}^{sj,\alpha}$.

7. Edge - Dependent Impedance Elements

where $\alpha = \mathrm{t\ or\ z}$, m is the mode number, and $\vec{\mathrm{w}}_{\mathrm{mi}}^{\mathrm{s}\alpha}$ is the testing function

The edge transition region is subdivided into a region on the BOT and on the cap surfaces, respectively (Fig. 2(b)). This subdivision is analogous to the two-region treatment of the junction region. Detailed derivation and summary of these elements are given in [13].

TABLE 1 .

Junction- Independent Impedance Elements. (Impedance matrix for the BOT surface, Z_{mn}^{ss} [8]

$$(Z_{mn}^{tt,tt})_{ij} \cong jk\square \sum_{p,q=1}^{4} \left\{ T_p^t\, T_p^t \cos(v_p - v_q) - \frac{1}{k^2}\dot{T}_p^t\, \dot{T}_q^t \right\} G_{mn}(p,q)$$

$$(Z_{mn}^{tt,zt})_{ij} \cong -\frac{m\pi\square}{kL} \sum_{p,q=1}^{4} \dot{T}_q^t\, T_p^z G_{mn}(p,q)$$

$$(Z_{mn}^{tt,zz})_{ij} \cong jk\square \sum_{p,q=1}^{4} T_p^z\, T_q^z \left\{ (1 - \frac{mn\pi^2}{k^2L^2})\ G_{mn}(p,q) + \bar{G}_{mn}(p,q) \right\}$$

where

$$\bar{G}_{mn} = (-1)^{m+n} G_{00} - (-1)^m G_{0n} - (-1)^n G_{0m}$$

$$G_{mn}(p,q) = L \int_0^2 d\pounds\ v_{mn}(\pounds)(\Delta t_p)(\Delta t_q) \frac{e^{-jkR_{pq}}}{R_{pq}}.\ p \neq q$$

$$v_{mn}(\pounds) = \begin{cases} \frac{1}{\pi}\left(1 - \frac{\pounds}{2}\right) cosnz\pounds\ , & m = n \\ \frac{1}{\pi}\frac{(-1)^{m-n+1}}{(n-m)\pi} S.n\left(\frac{n-m}{2}\right) z\pounds \cos\left(\frac{n-m}{2}\right)\pi\pounds, & m \neq n \end{cases}$$

$$G_{mn}(p,q) = 2L^2 \int_0^2 d\pounds\, e^{-jk\pounds} \left\{ v_{mn}(\pounds) \left[-jk\frac{\Delta t_p}{2L} + (t + jk\pounds) \ln\left(\frac{\Delta t_p}{2L} + \sqrt{\left(\frac{\Delta t_p}{2L}\right)^2 - \pounds^2} \right) - jk\pounds\left(\frac{2}{r\pounds} - 1\right) \right] + \pounds\left(\frac{1}{r\pounds} - 1\right) \dot{v}_{mn}(\pounds) \right\}.\ p \neq q$$

Impedance matrix for the BOT-wire interactions, Z_m^{sw}

$$(Z_m^{sw,t})_{i\pounds} \cong jk\square \sum_{p,\tau=1}^{4} \left\{ \frac{(\Delta x_\tau cosv_p + \Delta y_\tau sinv_p)}{\nabla\pounds_\tau} T_p^t T_\tau - \frac{1}{k^2}\dot{T}_p^t \dot{T}_\tau \right\} G_m(p,\tau)$$

$$(Z_m^{sw,z})_{i\pounds} \cong jk\square \sum_{p,\tau=1}^{4} \left\{ \frac{\Delta z_\tau}{\nabla \pounds_\tau} T_p^z \, T_\tau [G_m(p,\tau) - (-1)^m G_0(p,\tau)] + \frac{jm\pi}{k^2 L} \, T_p^z \, \dot{T}_\tau G_m(p,\tau) \right\}$$

where index τ is associated with the l-th wire segment and

$$G_{mn}(p,q) = \Delta t_p \nabla \pounds_\tau \int_L^L e^{-\frac{jmtz}{L}} \emptyset_{pq}(z)$$

TABLE 2 .

Junction- Dependent Impedance Elements. (BOT- junction impedance matrix, Z_m^{sj}: [8]

$$(Z_m^{sd,t})_i \cong \frac{jk\square}{4} \sum_{p,q=1}^{4} \left\{ sin\alpha_q \cos(v_p - v_d) \, T_p^t \left(\frac{a-b}{2}\right) - \frac{1}{k^2} \dot{T}_p^t \right\} G_{mn}(p,q)$$

$$(Z_m^{sd,z})_i \cong \frac{jk\square}{4} \sum_{p,q=1}^{4} \left\{ cos\alpha_q \, T_p^z \left(\frac{a-b}{2}\right) \left(G_{mn}(p,q) - (-1)^m G_0(p,q)\right) + \frac{jm\pi}{k^2 L} \, T_p^z G_{mn}(p,q) \right\}$$

where

$$\alpha_q = \frac{\pi}{2}(q-1) + \frac{\pi}{4} \; ; \tau_q = \frac{a+b}{2}$$

$$x_q = x_d + \tau_q sin\alpha_q cosv_d$$

$$y_q = y_d + \tau_q sin\alpha_q sinv_d$$

$$z_q = z_d + \tau_q cos\alpha_q$$

8. The Results

The voltage excitation [V] (i.e., right column vector in (7)) is specified by the location and electrical characteristics of the wire antenna on the body. The nonzero element of [V] corresponding to the segment of the wire that is actively fed. For an attached wire antenna , the junction voltage V^j is specified. For a parasitic radiator, on the other hand, $V^j = 0$. For simplicity, in the present discussion I exclude radiators on cap and edge regions. The formulation was used to predict the far fields radiated by wire antenna on various BOT configurations. Both active and passive wire radiators were considered on open as well as closed (capped) bodies. The unknown matrix column vector [I] of the current coefficients is determined once the applied excitation (voltage vector) is specified.

To illustrate the versatility and accuracy of this formulations for BOT, it was applied on the foregoing cylinder is shown in Fig. 3(a). The radiation pattern was predicted for this BOT. The comparison of measured and calculated data with the results [8] for the foregoing cylinder with a loop antenna are shown in Fig. 3(b). There is good overall agreement with in the shape and location of the major pattern lobes and nulls. The results for loop antenna mounted on the foregoing cylinder are shown in Fig. 3(b). The loop was 0.69λ long, offset $l_w = 0.138\lambda$. The feed-point was at the center of the cylinder. The effect of deleting the junction at point B in the BOT analysis for the yaw plane calculations also is shown.

The configurations tested included a cylinder, a cone-sphere shown in figs. 4-6.

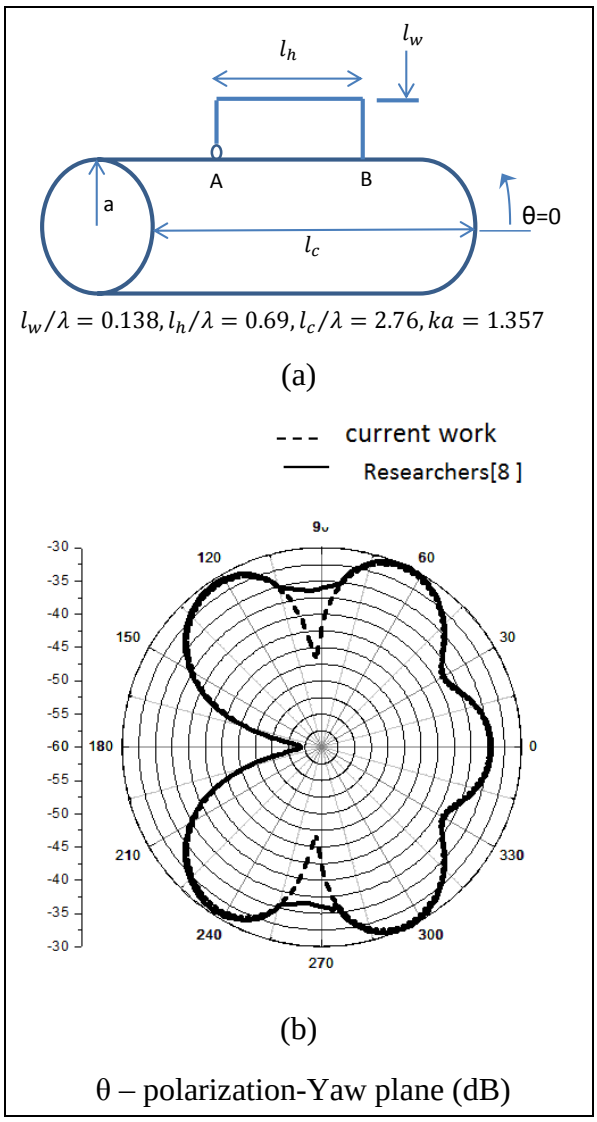

Fig. 3 Comparison current work and researchers work [8] computed Power radiation pattern for cylinder mounted antennas (loop antenna)

First, the simplest case was examined, namely monopoles on open cylinders. The validation baseline was the predictions using the analysis in [4]. Fig. 4 depicts the yaw plane pattern in θ polarization for opposing quarter-wave active and passive (parasitic) monopoles, mounted mid-point on an open cylinder having a ka=1.2 and 2.4 λ $long$. Next, a capped cylinder of length $l_c = 0.6\,\lambda\; and\; ka = 0.2$ with two attached quarter-wave elements was considered Fig.5 .The element at the cylinder midpoint was a base-fed monopole; the other attached element (midway between the active element and the cylinder end) was unfed (passive). The radiation pattern was computed with and without the effect of the junction (current) interaction at the base of the unfed element. The pattern is plotted in power using a linear (not decibel) scale and normalized to unity. The results in Fig.5 clearly indicate the crucially of including the junction interactions.

Fig. 6 is shown the radiation pattern for the cone-sphere with a loop antenna. The feed point was at the cone-sphere junction, and the total length of the loop was $0.2\,\lambda,\; and\; off-set\; 0.07\lambda$ from the surface of the cone-sphere. In the calculation two junctions were used on the loop, namely, one at the feed point and the other at the connection point to the cone-sphere surface.

9. Conclusions

The BOT-wire-junction problem has been formulated in terms of the electric-field integral equation and solved by method of moments. The present approach is applicable to analyses of the radiation characteristics of a variety of off-surface wire and loop radiators. By obvious extension, this method can be used to treat wire antennas attached to, or near, various curved and flat reflectors.

The information on surface current distribution is also useful in assessing the degree of electromagnetic coupling between monopoles in the case of multiple antennas.

Radiation pattern is shown distribution the energy from the antenna to the astrosphere. It is important for limiting the practical applications for antenna.

Antenna characteristics such as gain , directivity and efficiency may be computed.

The results are useful for impedance matching between transmission Line and antenna's input impedance.

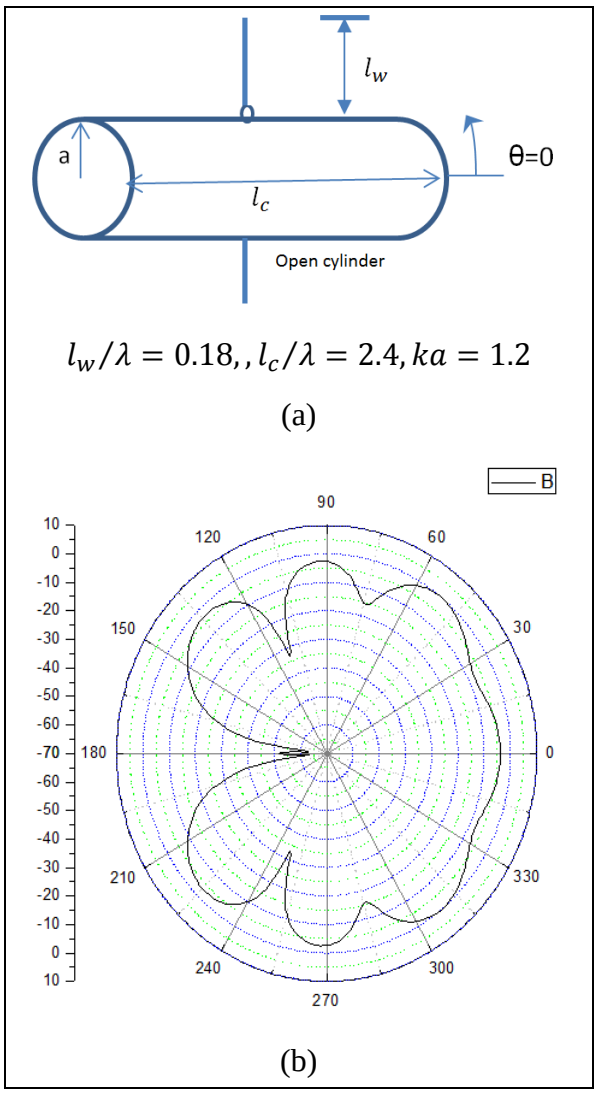

Fig. 4. Power radiation pattern for cylinder mounted antennas (opposing monopoles)

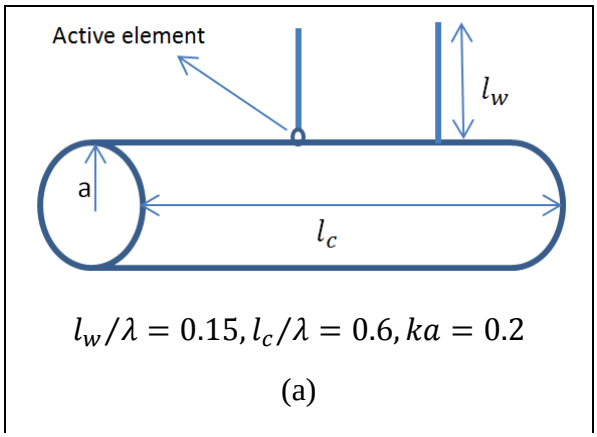

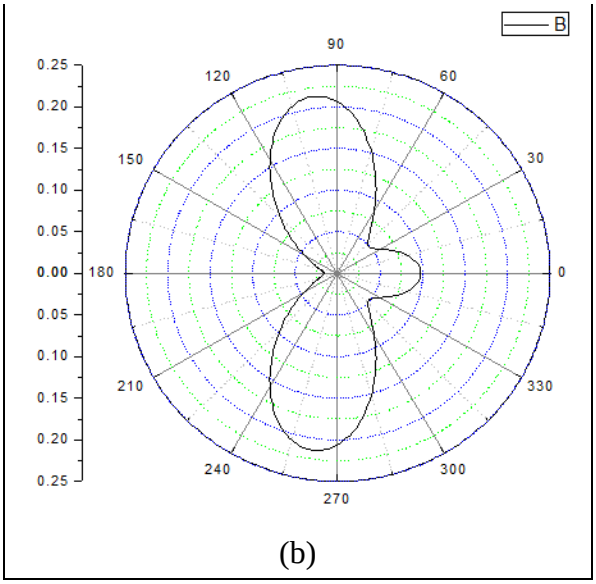

Fig. 5. Power radiation pattern for cylinder mounted antennas monopoles

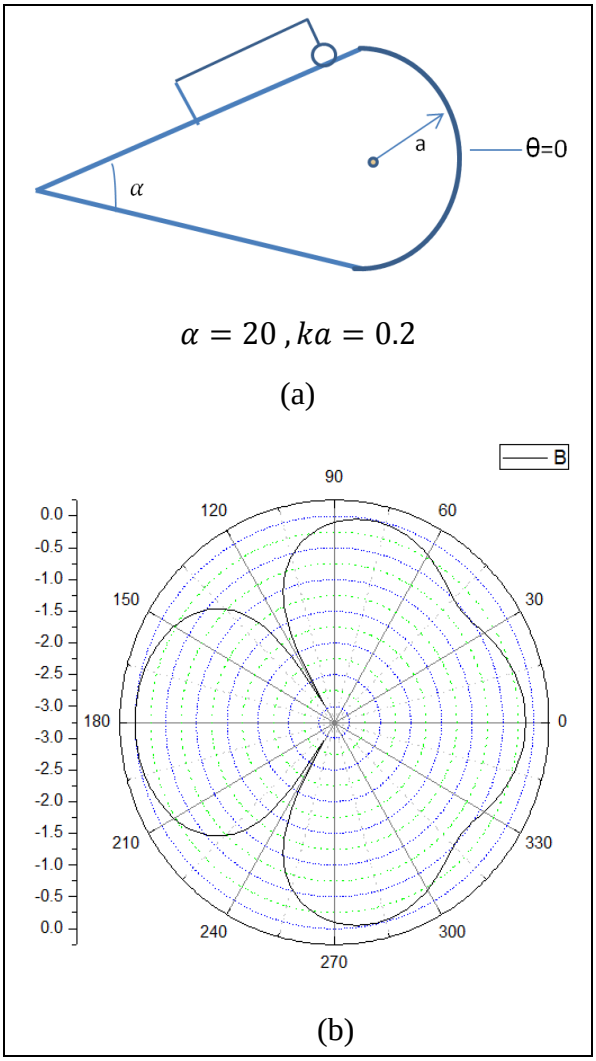

Fig. 6. Pitch-plane radiation pattern for cone-sphere with loop

10. Reference

[1] C. A. Balanis, "Antenna Theory Analysis and Design", John Wiley & Sons, Inc., Canada, 2005.

[2] W. C. Gibson," The Method of Moments in Electromagnetics", Chapman & Hall/CRC, Boca Raton, 2008.

[3] J. R. Mautz, " Scattering from loaded wire objects near a loaded surfaces of revolution, " Syracuse univ. Res. Crop., SURC TN 74-030. Jan. 1974.

[4] J. F. Shaeffer and L. N. Medgyesi-Mitschang, " Radiation from wire antennas attached to bodies of revolution: The junction problem," IEEE Trans. Antennas Propagat., vol. AP-29,p.479,1981.

[5] L. N. Medgyesi - Mitschang , " Scattering from thin plates and finite curved surfaces," in Proc. 1979 Int. Symp. Antennas Propagat., vol. I , p. 155.

[6] J. R. Mautz and R. F. Harrington, " Radiation and scattering from bodies of revolution," Appl. Sci. Res., vol. 20 , p. 405,1969.

[7] J. F. Shaeffer, " EM scattering from bodies of revolution with attached wire," IEEE Trans. Antennas Propagat., vol. AP-30 ,p.426,1982.

[8] L. N. Medgyesi – Mitschang," Formulation for wire radiations on bodies of translation with and without end caps," IEEE Trans. Antennas Propagat., vol. AP-31 ,p. 853,1983.

[9] A. W. Glisson and D. R. Wilton, " Simple and efficient numerical methods for problems of electromagnetic radiation and scattering from surfaces," IEEE Trans. Antennas Propagat., vol. AP-28, p. 593 ,1980.

[10] J. J. H. Wang," Numerical analysis of three-dimensional arbitrarily-shaped conducting scatters by trilateral surface cell modeling ."Radio Sci. , vol.13, p. 947, 1978.

[11] E. H. Newman and D. M. Pozar, " Electromagnetic modeling of composite wire and surface geometries," IEEE Trans. Antennas Propagat., vol. AP-26, p. 784 ,1978.

[12] R. F. Harrington, " Considerations for efficient wire/surface modeling," IEEE Trans. Antennas Propagat., vol. AP-28 ,p. 121,1980.

[13] L. N. Medgyesi - Mitschang and J. M. Putnam," Algorithm for surface of translation attached radiators (A-STAR)," RADC TR-82-113,vols. I-III, May 1982.